Features of intra-hamate vascularity and its possible relationship with avascular risk of hamate fracture

Zi-Run Xiao[1], Wei-Guang Zhang[2], Ge Xiong[1]

[1]Department of Hand Surgery, Beijing Jishuitan Hospital, Beijing 100035, China;
[2]Department of Anatomy and Histology, Peking University Health Science Center, Beijing 100191, China;
Zi-Run Xiao now works at Department of Orthopaedic Surgery, No. 988 Hospital of Joint Logistic Support Force.

Abstract

Background: The angiography with micro-computed tomography (micro-CT) has been proved its great advantages on investigating the intra-osseous vascularity of carpal bones. But few researches have focused on the intra-hamate vascularity. This study aimed to illustrate the intra-osseous arteries of the hamate and the relationship between the intra-hamate vascularity and the avascular risk of different types of hamate fractures.

Methods: Six normal cadaveric hamates were investigated with red lead (Pb_3O_4) micro-CT angiography. The intra-osseous arteries of specimens were clearly enhanced and the three-dimensional model was reconstructed. In order to study the features of the arterial entrances and intra-hamate vascularity, the diameters, quantities, locations of enhanced arteries, and the locations of transversal/proximal pole fracture lines on the body of the hamate were statistically compared. Besides, in order to analyze the relationship between intra-hamate vascularities and different hamate fractures, 127 cases of hamate fractures who presented in our hospital from March 2003 to June 2017 were retrospectively studied.

Results: A total of 94 cases were followed up (range: 4–37 months; mean: 12.4 months) effectively. The overall union rate of hamate fractures was as high as 92.6% (87 of 94 cases), while non-union of fracture on hamate hook was more common ($P = 0.031$). The arterial entrances were located around the dorsal, volar, radial, ulnar non-articular surfaces of the hamate body and the hook of the hamate. Generally, there were one to two trunk arteries on the volar non-articular surface and one to three trunk arteries on the dorsal non-articular surface. They formed one or two arterial arches, from which some branches were emitted and supplied the proximal parts. The intra-osseous vascularities of the hamate body were generally located in the radial part. The blood supply of the hook was mainly from the volar non-articular surface in most specimens. Hamate fractures could be classified into four types: fractures of the transversal/proximal pole, medial tuberosity, dorsal coronal of the hamate body, and fractures of the hamate hook.

Conclusions: This study showed new features of intra-hamate vascularity and the results will guide surgeons to reduce the vascular damage during the hamate fracture operations. The fracture lines of different types of hamate fractures may disrupt the intra-hamate arteries. The intra-hamate vascularities will have different influences on the avascular risks of different hamate fractures.

Keywords: Micro-computed tomography angiography; Intra-hamate arteries; Hamate fractures; Avascular risk

Introduction

Fractures of the hamate are relatively rare among carpal fractures.[1-3] The delay of diagnosis and inappropriate treatment may result in some complex complications, such as the obsolete sub-luxation of the 4/5th carpometacarpal joints, persistent pain and decreased griping force. Especially, the delayed union or non-union of a hook fracture may cause irritation of the tendon and the ulnar nerve which may result in more serious complications such as rupture of the tendon and ulnar nerve injury.[2,4,5]

Gelberman *et al*[6,7] systematically studied the intra-osseous and extra-osseous vascularity of all carpal bones and established the anatomical basis of the wrist joint and each carpus. But unfortunately, the description of each carpus was quite brief (only 115 words for the hamate). Failla[8] studied the hamate hook vascular foramina under a microscope, in which just the foramina instead of intra-osseous vessels were analyzed, and summarized that the blood supply feature of the hook might be a factor of hamate hook non-union. But the foramina distribution cannot accurately illustrate the blood supply for the carpal bone, since our previous research[9] showed that there were always some foramina which contained no artery. Therefore, it was really a pity that the authoritative work was still citing these results to explain the problems of fracture healing.[10]

Access this article online

Quick Response Code:

Website: www.cmj.org

DOI: 10.1097/CM9.0000000000000417

Correspondence to: Prof. Ge Xiong, Department of Hand Surgery, Beijing Jishuitan Hospital, No.31 Xinjiekou East St., Xicheng District, Beijing 100035, China
E-Mail: dr_xiongge@hotmail.com

Chinese Medical Journal 2019;132(21)

Received: 24-02-2019 **Edited by:** Ning-Ning Wang

Recently some studies have focused on the intra-osseous arterial system in the lunate, scaphoid, and capitate bones with micro-computed tomography (micro-CT) angiography and obtained many valuable results.[9,11,12] With the aid of the modern digital technology, more details about the intra-osseous artery system can be obtained. The more details that are observed, the more clinical significances are discovered. The purpose of this study was to illustrate the intra-osseous arteries of the hamate with this new method and to discuss the relationship between the intra-hamate vascularity and the avascular risk of different types of hamate fractures.

Methods

Ethical approval

The study was conducted in accordance with the *Declaration of Helsinki* and was approved by the local ethics committee of Beijing Jishuitan Hospital (No. 201707-17). All the cadaver specimens were provided by Peking University Health Science Center and donated voluntarily by donors.

Angiography with red lead

Sixty grams of Pb_3O_4 powder was ground, filtered through a 300-mesh screen (diameter of about 48 μm), and divided into three equal parts. Each part was mixed with 10, 20, or 30 mL of turpentine to produce three suspensions.

Six fresh cadaver upper limbs from three donors (a 55-year-old woman, a 60-year-old man, and a 65-year-old man) were studied. Radiography was used to assess and exclude diseased carpi. The limbs were completely thawed at room temperature and the brachial artery was dissected. Pb_3O_4 suspensions were injected into the brachial artery from a low concentration to a high concentration until the tips of the fingers turned red. Then the artery was ligated. All limbs were fixed in 10% formalin for 48 h.

Micro-CT scanning

After fixation, the hamate was removed from the wrist and the soft tissues around it were stripped as completely as possible. All specimens of hamates were scanned with micro-CT (SkyScan 1172, Kontich, Belgium; Scanning conditions: 100 kV, 90 μA, resolution 12 μm) and three-dimensional (3D) images were constructed. The constructed images were converted into the Digital Imaging and Communications in Medicine (DICOM) format (a readable format for software) and loaded with Mimics software (Version 17.0, Materialise NV, Leuven, Belgium). By observing the images of the nutrient foramina on the cortices of the hamate images layer by layer, the number, diameter, and location of the nutrient foramina, and the enhanced arteries were recorded. 3D images of enhanced arteries and the whole hamate were reconstructed and the intra-osseous arterial pattern was observed on the transparent hamate image from different directions.

Classification and outcomes of hamate fractures

Over the past 13 years (from March 2003 to June 2017), there were 127 patients who suffered from the hamate fractures in Beijing Jishuitan Hospital. To illustrate the relationship between the avascular risk of hamate fractures and the intra-hamate vascularity, all these patients were retrospectively studied.

All these cases were classified according to their radiograph and/or CT images from the time of the initial diagnosis. Treatment strategies (surgical or conservative) were established according to both surgeon's suggestions and the patients' requirements. Patients were followed up every 2 to 4 weeks and the bone union was evaluated with radiograph and/or CT images. Generally, the callus healing could be found in 6 to 8 weeks. The non-union was defined if the fracture lines were still visible for more than 6 months. After fracture healing, the follow-up could be continued as long as possible to facilitate analysis of long-term outcome.

Finally, 33 patients were lost to follow-up despite extensive attempts. The outcomes of remaining 94 cases (74% of all cases reviewed in this study) were recorded and analyzed.

Observation and measurement

We marked the location of nutrient arteries and measured the diameter of them on each cortical surface. For the body of the hamate, the main trunk and non-trunk arteries were labeled and counted. In order to describe and quantify the position of the arterial entrance of the body of the hamate, we drew a longitudinal line from the central point on the central ridge between the 4th and 5th carpometacarpal articular surface to the proximal pole of the hamate (the most prominent central point of the margin of the proximal articular surface) in the 3D model and recorded the distance (recorded as distance A). The vertical projection point of the entrance position on this line was set. Then the distances (recorded as distance B) between the proximal pole and vertical projection point were calculated. In order to fully describe the characteristics of arteries, the data were measured to a precision of 12 μm. We defined the ratio of this distance B to A as the location value of each entrance point on the body of hamates (some location values were slightly greater than 100% because some arterial entrances were more distal than the distal reference point). All the location values of the trunk and non-trunk arterial entrance points were calculated and recorded. For the hook of the hamate, the above method was not appropriate, so we separately observed and described the intra-osseous arteries of the hook.

In the cases of transversal/proximal pole fractures of the hamate body, the distances between fracture lines to the proximal pole were measured on radiographs or CT images. We also defined the ratio of this distance to the whole length of the hamate body as the location value of the fracture lines.

Statistical analysis

All the data were checked with the Shapiro-Wilk test for normality. The data of diameters, quantity of arteries on the volar/dorsal surface of the hamate body did not show a normal distribution, so the data are presented in the form of the median (interquartile range [IQR]: 25% to 75%

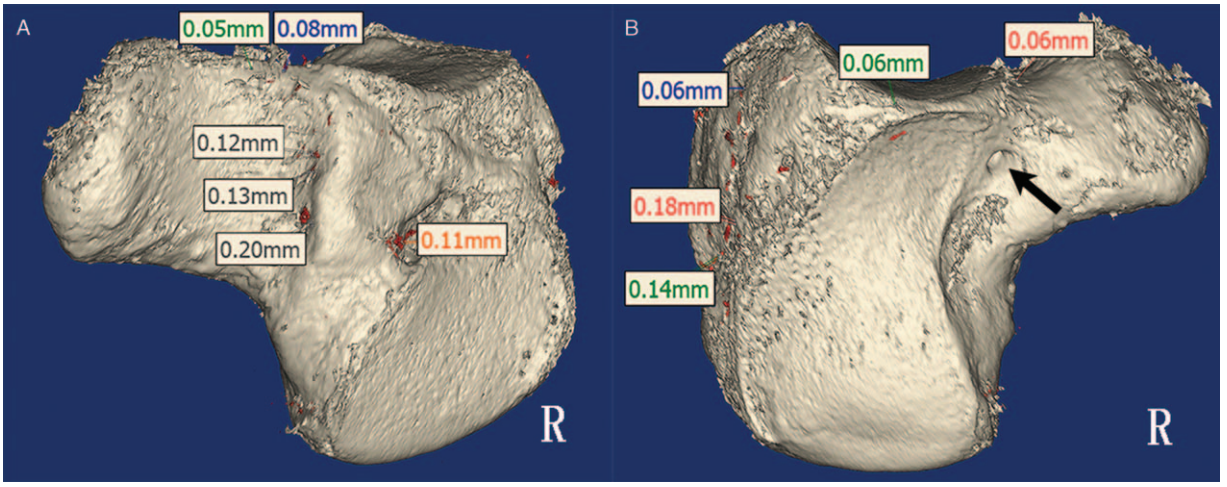

Figure 1: The three-dimensional model of one hamate shows the locations where arteries enter the hamate bone and their diameters. (A) The volar and radial sides of the hamate. (B) The dorsal and ulnar sides of the hamate. The black arrow shows an obvious nutrient foramen on the ulnar base of the hook, in which there is no enhanced artery. R: Right.

Table 1: The location distribution of the nutrient foramina and enhanced arteries of the hamate.

	Sample 1		Sample 2		Sample 3	
Location distribution of the nutrient foramina	**R**	**L**	**R**	**L**	**R**	**L**
Volar						
Total, *n*/*N*	3/7	3/5	3/4	2 /2	3/3	4/5
Trunk artery, *n*	1	1	2	1	1	1
Dorsal						
Total, *n*/*N*	3/6	7/8	15/16	13/15	9 /12	8/10
Trunk artery, *n*	1	2	3	1	2	1
Radial, *n*/*N*	3/5	1/3	1/3	4/5	2/3	1/3
Ulnar, *n*/*N*	1/1	0/0	1/1	0/0	0/0	0/0
Hook, *n*/*N*	3/6	3/5	3/3	4/4	2/4	6/10

N: The number of the nutrient foramina; *n*: the number of the enhanced arteries; L: Left; R: Right.

quartiles) and the Mann-Whitney *U* test or Wilcoxon signed-rank test was used. The data of location values of arteries and the location values of transversal/proximal pole fracture lines on the body of the hamates conformed to a normal distribution, so the data were presented in the form of mean ± standard deviation and the *t* test (two-tailed) was used to compare the significance. All data were analyzed using SPSS 20.0 statistical software (IBM, Chicago, IL, USA). Statistical significance was set at a $P \leq 0.05$.

For the retrospective study of 127 hamate fracture cases, the Fisher exact test was used to compare the difference of non-union rate in different fracture types.

Results

Features of arterial entrances and intra-hamate vascularity

The nutrient foramina were generally located around five areas: the dorsal non-articular surface, the volar non-articular surface, the radial non-articular surface, the ulnar non-articular surface and the hook [Figure 1]. Some foramina (41/149, 27.5%) did not contain an artery [Table 1]. The major vascularity of the hamate was from dorsal and volar non-articular surfaces. There were one to two trunk arteries on the volar non-articular surface and one to three arteries on the dorsal non-articular surface. In most specimens (5/6), the trunk arteries from the dorsal and volar sides formed one or two arterial arches through their anastomoses. Some branches arose from these arterial arches and supplied the proximal parts of the hamate. In the other specimen (1/6) no obvious anastomosis of trunk arteries was found. There were some arteries around the radial non-articular surface, but they were usually small ones. On the ulnar non-articular surface, only one small artery in 2/6 specimens was found while none was found in the other 4/6 specimens.

Importantly, when we divided the hamate into two parts with a sagittal plane through the proximal pole and central ridge between the 4th and 5th carpometacarpal joint surface, most arterial entrances (including all trunk arteries) and the intra-osseous vascularity were located in the radial part [Figure 2A–D].

Classification and outcomes of hamate fractures

Based on the radiograph and/or CT data from all 127 cases of hamate fractures reviewed in this study, they were divided into four types: fractures of transversal/proximal pole, medial tuberosity, dorsal coronal of the hamate body and fractures of the hamate hook. The coronal fractures of

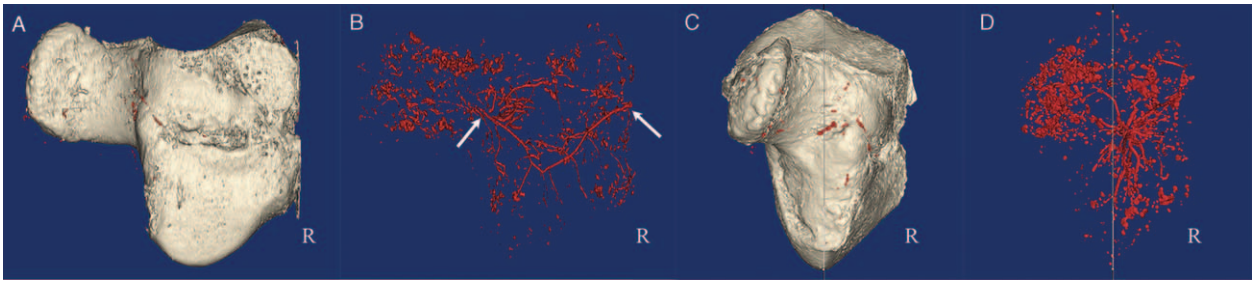

Figure 2: A three-dimensional image of a hamate (A) and the three-dimensional image of intra-osseous arteries (B) shows the features of the intra-osseous arteries in the hamate body. The trunk arteries (white arrows) enter the volar and dorsal sides and form an arterial arch. Then some branches are emitted from the arterial arch and supply the proximal part of the hamate. A three-dimensional image of the hamate (C) and the three-dimensional image of the intra-osseous arteries (D) show a special feature of intra-osseous vascularities. When a sagittal plane was set through the proximal pole and central ridge between the 4th and 5th carpometacarpal joint surface, most of the intra-osseous vascularities of the hamate body are located in the radial part. R: Right.

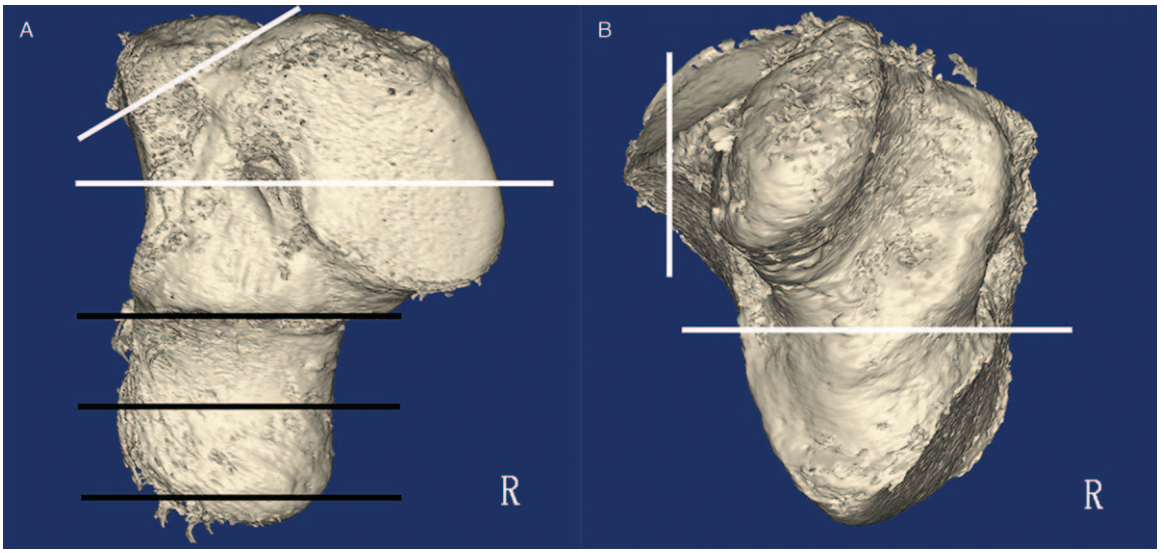

Figure 3: The classification of hamate fractures. (A) The white lines show the dorsal coronal fracture of the hamate body, which is sub-divided into dorsal oblique fractures (the upper short white line) and splitting fractures (the lower long white line). The black lines show the hamate hook fractures. The three black lines are the three sub-types (basal fracture, middle part fracture, and the tip fracture), respectively. (B) The white lines show the fractures of transversal/proximal pole (the transversal white line) and medial tuberosity (the longitudinal white line). R: Right.

the hamate body were sub-divided into two types: dorsal oblique fractures and splitting fractures [Figure 3].

The mean follow-up time for the 94 cases was 12.4 months (range: 4.0–37.0 months). Sixty-one were male and 33 were female, with an average age of 34.4 years (from 16.0 to 67.0 years). Although not all patients underwent surgical intervention, the union rate of hamate fracture was still up to 92.6% (87 of 94 cases). The non-union rate was only 5.3% (5 of 94 cases) and the remaining two cases ended up with malunion.

From the view of classification, the fracture of the hamate hook has a significantly high rate of non-union ($P = 0.031$). But the patients were generally satisfied with the results on the last follow-up. The classification results of hamate fractures are shown in Table 2.

Intra-osseous vascularity in the hamate hook

In most specimens (5/6), the major blood supply of the hook was from the volar non-articular surface. Some tiny arteries around the distal and ulnar base of the hook could be identified. In the other specimen there was a trunk artery entering the hook from its tip and running to the base of the hook. The distribution features of intra-osseous arteries in the hamate hook can be divided into three patterns.

Pattern 1: An artery, which was slightly thinner than trunk arteries, entered the volar non-articular surface and then ran to the tip underneath the radial cortex of the hook. Some other small arteries were found at the distal hook and the ulnar side of the hook base. This type was the most common and was found in four of the six specimens [Figure 4A and 4B].

Pattern 2: Two branches from the volar trunk arteries were identified. They ran to the tip underneath the radial cortex of the hook. Some small arteries were also found. This type was found in one specimen [Figure 4C and 4D].

Pattern 3: The arteries from the volar non-articular surface were very small. There was one trunk artery entering the hook from the ulnar tip and running to the base of the hook. Some other small arteries were found around the

Table 2: The classification and outcome of hamate fractures.

Fracture types	Follow-up, *n*	Surgical cases (*n* = 79)			Conservative cases (*n* = 15)			Total non-union, *n* (*n*/*N*)
		Union	Malunion	Non-union, *n* (*n*/*N*)	Union	Malunion	Non-union, *n* (*n*/*N*)	
Hook	27	15	0	1 (1/16)	8	0	3 (3/11)	4 (4/27)*
Tip	2	0	0	none	1	0	1 (1/2)	1 (1/2)
Waist	12	5	0	1 (1/6)	4	0	2 (32/6)	3 (3/12)
Base	13	10	0	0	3	0	0	0
Dorsal coronal fracture	60	58	0	0	0	1	1 (1/2)	1 (1/60)
Splitting	6	6	0	0	0	0	none	0
Dorsal oblique	54	52	0	0	0	1	1 (1/2)	1 (1/54)
Transversal/proximal pole fractures	5	4	1	0	0	0	none	0
Medial tuberosity	2	0	0	none	2	0	0	0
Total number	94	77	1	1 (1/79)	10	1	4 (4/15)	5 (5/95)

*The non-union rate of hook fracture is significantly higher than dorsal coronal fracture ($P = 0.031$).

hook. This pattern was only found in one specimen [Figure 4E and 4F].

In the two specimens of sample 1 (a 55-year-old woman), the contrast agents were found accumulated inside the hook of the hamate. But, this situation did not exist in other specimens. The accumulated contrast agents appeared as continuous small lumps, like grapes [Figures 2B and 4B].

Intra-osseous vascularity of hamate body

There were 18 arteries from the volar non-articular surface. The median quantity and diameter of all 18 arteries were 3.00 mm (IQR: 2.80–3.30 mm) and 0.13 mm (IQR: 0.09–0.16 mm), respectively. There were 55 arteries from the dorsal side and the median quantity and diameter of them were 8.50 mm (IQR: 6.00–13.50 mm) and 0.11 mm (IQR: 0.08–0.14 mm), respectively. The difference of the arterial diameter between the volar and dorsal sides was not significant based on the Mann-Whitney *U* test ($Z = -0.783$, $P = 0.434$). However, the quantity of arteries from the dorsal side was significantly larger than that from the volar side based on the Wilcoxon signed-rank test ($Z = -2.032$, $P = 0.042$).

There were seven trunk arteries on the volar side and ten trunk arteries on the dorsal side. The median quantity was 1.00 mm (IQR: 1.00–1.30 mm) for the volar side and 1.50 mm (IQR: 1.00–2.30 mm) for the dorsal side, while the median diameter was 0.16 mm (IQR: 0.14–0.20 mm) for the volar side and 0.18 mm (IQR: 0.17–0.21 mm) for the dorsal side. However, there were no significant differences for both the quantity ($Z = -1.732$, $P = 0.083$,) and diameter ($Z = -1.430$, $P = 0.153$) between the two sides.

The mean location value of trunk and non-trunk arteries (including the arteries around the radial and ulnar surfaces) was 67% ± 11% and 80% ± 17%, respectively. The difference was significant based on the independent sample *t* test ($t = -3.091$, $P = 0.003$). Most location values of the trunk (94%, 16/17) and non-trunk (96%, 67/70) arteries were larger than 50%.

We recorded the location value of the most proximal artery and the most proximal trunk artery in each specimen. The mean location value of the most proximal arteries was 47% ± 11%, whereas the mean location value of the most proximal trunk arteries was 58% ± 13%. But the difference was not significant ($t = 2.254$, $P = 0.074$) [Table 3].

In the specimens of transversal/proximal pole fractures of the hamate body, the mean location value of fracture lines was 45% ± 5%. This value was significantly smaller than the mean value of most proximal trunk arteries in our specimens with angiography ($t = -2.478$, $P = 0.031$).

Discussion

New findings of intra-hamate vascularity

After Lee[13] first studied the intra-osseous vascularity of the lunate with the Spalteholz method, Panagis *et al*[7] systematically investigated the intra-osseous vascularity of all carpal bones and established the anatomical basis of the wrist arterial system. Failla's[8] study concerned the distribution of vessel entrances around the hamate hook, but the inadequacies of this study were obvious. The research only focused on the foramina distribution instead of intra-osseous vessels. According to our observations, almost 28% of foramina contained no artery in the hamates. So the results of the foramina distribution cannot accurately reflect the artery distribution. Recently the latest studies about the intra-osseous arterial system in scaphoid, lunate, and capitate bones with micro-CT angiography demonstrated many valuable results and confirmed the feasibility and reliability of the new angiography method.[9,11,12,14]

Panagis's research[7] on the vascularity of the carpal bone is still fundamental. But their descriptions about intra-hamate vascularity were quite simple as follows. Dorsally, three to five vessels entered the non-articular surface and branched in all directions. These branches supplied the dorsal 30% to 40% of the bone. Palmarly, the hamate's pre-dominant blood supply was supplied by one large artery entering through the

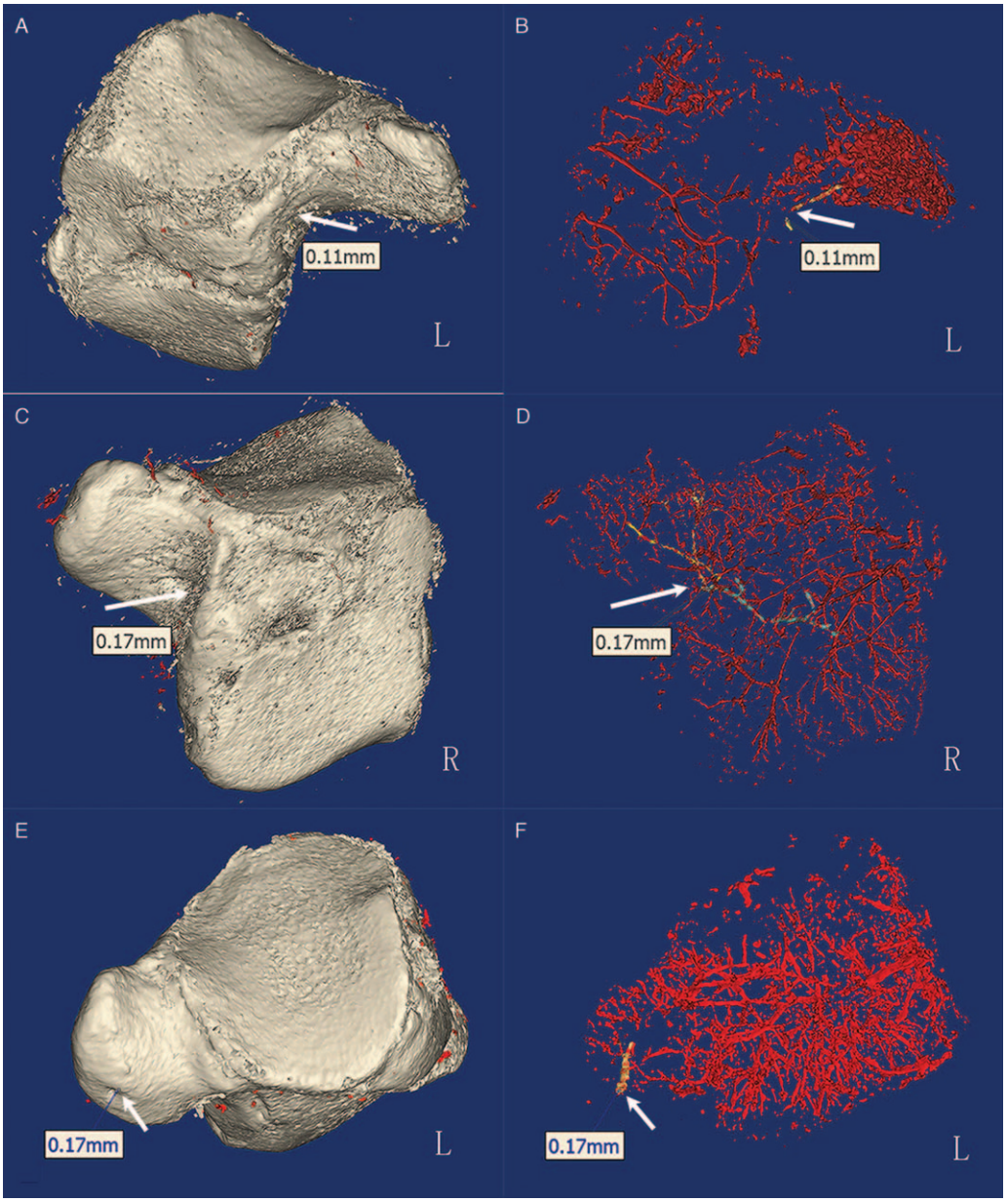

Figure 4: The three intra-osseous vascularity patterns of the hamate hook. (A) and (B) The first pattern: The white arrow shows an artery supplying the hook from volar surface of the body and this artery is constant in this type. The other arteries around the hook are usually inconstant. The contrast agent accumulation inside the hook is obvious in this specimen. (C) and (D) The second pattern: The white arrow shows a trunk artery (highlighted in blue) on the volar surface of the body. Two branches (highlighted arteries in yellow) are emitted from the trunk and supply the hook. (E) and (F) The third pattern: The white arrow shows a trunk artery on the tip of the hook. L: Left; R: Right.

Table 3: The location value of the most proximal arterial entrances.

	Sample 1				Sample 2				Sample 3			
	R		L		R		L		R		L	
Parameters	All	Trunk	All	Trunk	All	Trunk	All	Trunk	All	Trunk	All	Trunk
Location value (%)	57	69	57	57	34	34	33	67	48	58	52	64
Diameter (mm)	0.07	0.16	0.18	0.18	0.16	0.16	0.08	0.20	0.11	0.20	0.16	0.14

L: Left; R: Right.

radial base of the hook. Within the bone, it branched and formed significant anastomoses with dorsal vessels in 50% of specimens. The vascularity of the hook was consistently provided by one to two small vessels entering through the medial base and the tip of the hook. These two vessels anastomosed with each other in each specimen but, in the majority of specimens, failed to anastomose with the blood vessels of the body of the hamate.[7]

However, our research has obtained some important and different results: (1) The blood supply from the dorsal side may be dominant because the number of dorsal arteries is significantly larger than it on the volar side; (2) The rate (five of six specimens) of existence of anastomoses between the trunk arteries from dorsal and volar sides is much greater than Panagis's observation (50%); (3) Most of the arterial entrances and intra-osseous vascularity are located in the radial part and the blood supply of the ulnar part and proximal part is relatively poor, which is never reported before; (4) There are many thin arteries entering the hamate from the radial non-articular surface and the ulnar surface. But they are usually small and inconstant; (5) All arterial entrances are located around the ligaments, such as the capitohamate ligament, deep capitohamate ligament, carpometacarpal ligament, and transverse carpal ligament. This arterial distribution pattern can also be seen in other carpal bones.[9,11] In this way, the arteries are well protected by the rigid ligaments.

The accumulation of the contrast agent in the hamate hook was not reported in previous studies. The contrast agents demonstrated grapes-like continuous small lumps, which were more likely physiological blood sinuses rather than pathological bleeding. Especially, this situation was found bilaterally in one sample. The intra-osseous blood sinus is quite salient in the red marrow, which is very rare in a normal adult. But some studies have proved that the reconversion of yellow marrow to red marrow could occur in adults under many conditions, such as obese women who smoke heavily,[15,16] non-Hodgkin's lymphoma,[17] or hematopoietic growth factors.[18] Unfortunately, the life history of this donor is unclear. Further research, if there are complete life histories of this donor, will help us to explain this phenomenon.

Possible relationship between the avascular risk of hamate fractures and intra-hamate vascularity

Xiong *et al*[2] concluded the clinical classification of hamate hook fractures. For hamate body fractures, the classification methods are not unique.[19,20] Some authoritative works[1,10] sub-divide the hamate body fractures into four types: fractures of proximal pole, medial tuberosity, sagittal oblique, and dorsal coronal. The sagittal oblique fractures were image-based classification. We reviewed the literature but found no reported typical sagittal hamate fracture cases. All the literatures just quoted the description from Milch.[20] According to our observation of hamate fractures, we believe that the sagittal oblique type should be classified as a transversal fracture, which mainly involves the proximal part of the hamate. So we divided the hamate fractures into four types: fractures of transversal/proximal pole, medial tuberosity, dorsal coronal of the hamate body, and fractures of the hamate hook.

In the past, plaster immobilization might be used to deal with the acute cases of hook fractures, but the healing rate was not ideal.[21] The feature of vascularity of the hook was considered as a possible key factor of hook fracture non-union.[1,8] Our study has demonstrated that the blood supply from the volar non-articular surface is more important for the hamate hook than in the previous concept, and only in a few specimens, the trunk artery on the tip of hook was dominant with some small arteries from the base of the hook supplying the basal part. This feature may have different influences on different locations of hook fractures. Obviously both the basal part and the tip of the hook have more blood supply than the middle part. We believe that this is a very important factor which led to a significant higher fracture non-union rate for middle part fractures compared with the basal fractures.[2,4] The fractures of tip of the hook were generally avulsion fractures and the symptoms were always mild. But the middle part fractures of the hook may result in the complications of tear or disruption of flexor tendons of the ring and little fingers.[22] The statistical analysis has shown the hook fracture has a statistically significant high non-union rate than other fracture types of hamate, which was consistent with the feature of vascularity. In our study, we observed that the trunk arteries of the hook were generally located on the radial side and the tip of the hook, so using a dorsal approach or medial approach for open reduction and internal fixation is recommended.[23] The intra-osseous arteries of the hook will be protected if the screw is centrally placed.

Coronal fractures of the hamate body are often the results of axial forces from metacarpi, so this type is usually combined with sub-luxation or dislocation of the 4/5th carpometacarpal joint.[24] Ebraheim *et al*[25] proposed a classification for coronal body fractures. However, according to the intra-hamate vascularity, it is more appropriate to sub-divide this fracture into two sub-types: splitting fractures involving injuries of intra-osseous trunk arteries, and dorsal oblique fractures not involving injuries of intra-osseous trunk arteries. This classification method is similar to Hirano and Inoue's[19] work. Although the splitting fracture line can massively disrupt the anastomoses of the trunk arteries, the volar and dorsal fragments can be well supplied by the volar and dorsal trunk arteries, respectively. If the fracture line is limited to a small dorsal part such as the dorsal oblique fracture, it can hardly influence the main blood supply of the hamate body, but for the small fragment, some non-trunk arteries can also provide the blood supply [Figure 5]. This might be the reason that most of coronal fractures of the hamate body generally have good outcomes after surgical intervention.[25,26] However, the stable fixation of the fragment is still pivotal. The internal fixed screws should be centrally placed but slightly ulnar to prevent damage of the main intra-osseous arteries.

The fracture lines of transversal/proximal pole fractures are usually located more proximal than the trunk arteries according to our result [Figure 6A and 6B]. The blood supply of the proximal part is retrograde and poor. So there should be a high avascular risk for transversal/proximal pole fractures. But studies on isolated transversal and proximal pole fractures of the hamate are so rare that the clinical healing rate of these fractures is unclear. However, according to our follow-up results and the published researches of complex carpal injuries with transhamate fractures, the outcomes were generally good.[27,28,29] It was assumed that the tough ligament

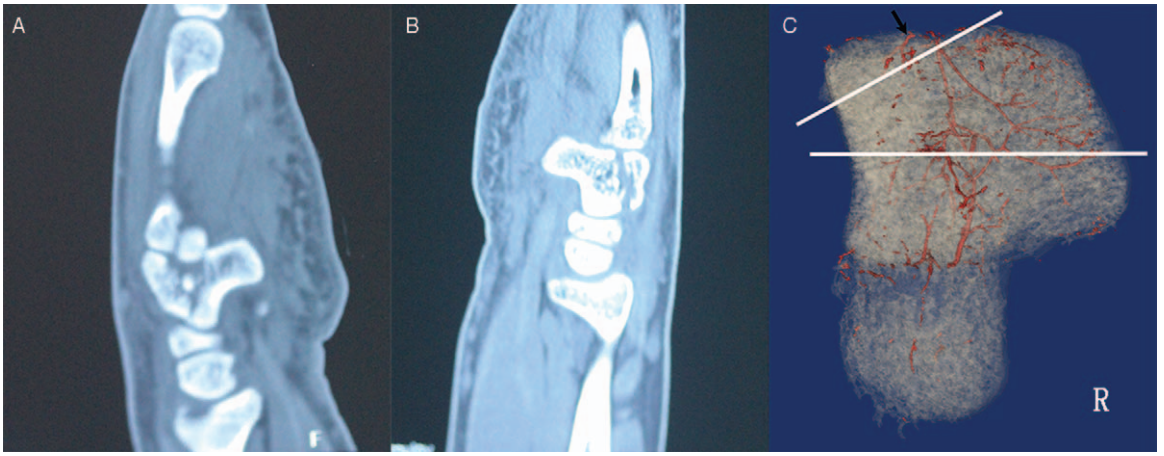

Figure 5: The influence of a dorsal coronal fracture on intra-hamate vascularity. (A) The splitting fracture will disrupt the anastomoses of the trunk arteries of the hamate body. (B) The dorsal oblique fracture may have limited influence on the intra-osseous arteries. (C) The white lines show the different locations of two types of a dorsal coronal fracture. The black arrow shows a non-trunk artery in the dorsal oblique fracture fragment. R: Right.

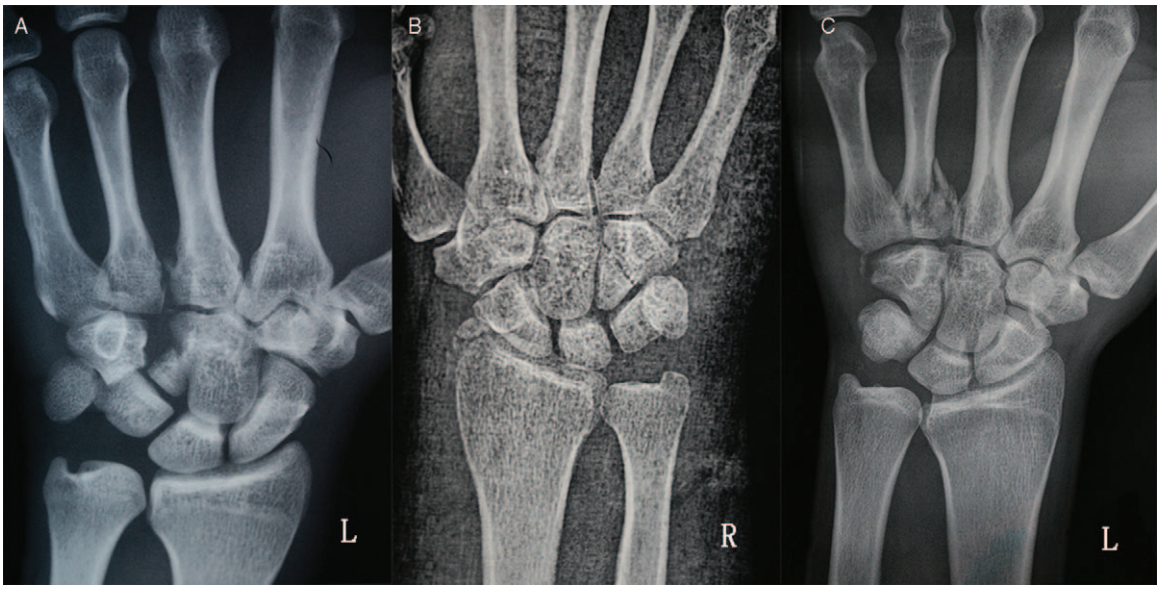

Figure 6: The other three fracture types of hamate body. (A) The proximal pole fracture and dislocation of the hamate. (B) The transversal fracture of the hamate. (C) The medial tuberosity fracture of the hamate. L: Left; R: Right.

connecting the capatite will provide rigid stability of hamate fractures.[28] In addition, the axial load helps to maintain the stability of transversal fractures. Also, unlike lunate fractures and proximal fractures of the scaphoid, the proximal part of the hamate is not a stress concentrating location of the wrist. It is less likely to cause a collapse of the fragment.[12,30]

Finally, the medial tuberosity fracture of the hamate body is a rare type of hamate injury. This type is usually caused by a direct blow to the ulnar side of the wrist [Figure 6C]. Although there are some non-trunk arteries located around this area, they are usually inconstant and small. We believe that the influence to the intra-osseous vascularity of this fracture type is limited. Generally the fracture fragments are small and the outcomes are good. Conservative immobilizations are recommended for this type of fracture.

At present, it is impossible to illustrate intra-osseous arteries for the hamate fracture patients *in vivo*. So it is hardly to obtain the direct evidence of the relationship between the fractures and intra-hamate vessels. But we found there were one to three constant trunk arteries from both volar and dorsal sides in each hamate sample. The abundant blood supply obviously contributes to the high healing rate of fracture of the hamate body. As to the fracture of hamate hook, the feature of intra-osseous arteries of hamate hook is highly correlated with the non-union rate of different type of the fracture.

The new feature of intra-hamate vascularity we obtained is more abundant than the previous studies. However, it is a pity that our sample size is still not big enough to well establish a classification for the intra-hamate arterial system. But we have obtained many new and interesting results, and this can lead to some significant instructive

clinical and treatment recommendations. A larger sample size is needed to confirm our classification and extend our understanding for the relationship of arterial patterns between different sides, genders, and ages. Otherwise, some spurious significance may be obtained.[31] We believe that our research can help hand surgeons take the features of intra-hamate vascularity into full consideration to properly assess and avoid damage of the intra-osseous arterial system when they deal with a hamate fracture in their practices.

Acknowledgement

The authors thanks to Dr. Edward C. Mignot from Shandong University, for linguistic advice.

Funding

This study was supported by the grant from the Peking University Medicine Information Foundation (No. BMU20160600).

Conflicts of interest

None.

References

1. Suh N, Ek ET, Wolfe SW. Carpal fractures. J Hand Surg Am 2014;39:785–791. doi: 10.1016/j.jhsa.2013.10.030.
2. Xiong G, Dai L, Zheng W, Sun Y, Tian G. Clinical classification and treatment strategy of hamate hook fracture. J Huazhong Univ Sci Technolog Med Sci 2010;30:762–766. doi: 10.1007/s11596-010-0654-7.
3. Bernstein RA. Are hamate fractures common? Letter regarding "carpal fractures" article. J Hand Surg Am 2014;39:2344. doi: 10.1016/j.jhsa.2014.08.026.
4. Xiong G. Hook of hamate fractures: location and tendon rupture. J Hand Surg Am 2014;39:175–176. doi: 10.1016/j.jhsa.2013.11.020.
5. Yamazaki H, Kato H, Nakatsuchi Y, Murakami N, Hata Y. Closed rupture of the flexor tendons of the little finger secondary to non-union of fractures of the hook of the hamate. J Hand Surg Br 2006;31:337–341. doi: 10.1016/j.jhsb.2005.12.015.
6. Gelberman RH, Panagis JS, Taleisnik J, Baumgaertner M. The arterial anatomy of the human carpus. Part I: the extraosseous vascularity. J Hand Surg Am 1983;8:367–375. doi: 10.1016/s0363-5023(83)80194-4.
7. Panagis JS, Gelberman RH, Taleisnik J, Baumgaertner M. The arterial anatomy of the human carpus. Part II: the intraosseous vascularity. J Hand Surg Am 1983;8:375–382. doi: 10.1016/s0363-5023(83)80195-6.
8. Failla JM. Hook of hamate vascularity: vulnerability to osteonecrosis and nonunion. J Hand Surg Am 1993;18:1075–1079. doi: 10.1016/0363-5023(93)90405-R.
9. Xiao ZR, Zhang WG, Xiong G, Zhang YL. Three-dimensional intralunate arteries visualization with red lead (Pb3O4) angiography. Chin Med J 2017;130:2575–2578. doi: 10.4103/0366-6999.213909.
10. Wolfe SC, Hotehkiss RN, Pederson WC, Kozin SH. Greens's Operative Hand Surgery. 6th EdnPhiladelphia: Churchill Livingstone; 2010. 1814.
11. Xiong G, Xiao ZR, Zhang WG. Vascular anatomy of the capitate determined by micro-computed tomography angiography. J Hand Surg Eur Vol 2017;42:966–967. doi: 10.1177/1753193417714400.
12. Xiao Z, Xiong G, Zhang W. New findings about the intrascaphoid arterial system. J Hand Surg Eur Vol 2018;43:1059–1065. doi: 10.1177/1753193418758890.
13. Lee ML. The intraosseus arterial pattern of the carpal lunate bone and its relation to avascular necrosis. Acta Orthop Scand 1963;33:43–55. doi: 10.3109/17453676308999833.
14. Kadar A, Morsy M, Sur YJ, Laungani AT, Akdag O, Moran SL. The vascular anatomy of the capitate: new discoveries using micro-computed tomography imaging. J Hand Surg Am 2017;42:78–86. doi: 10.1016/j.jhsa.2016.12.002.
15. Gonzalez FM, Mitchell J, Monfred E, Anguh T, Mulligan M. Knee MRI patterns of bone marrow reconversion and relationship to anemia. Acta Radiol 2016;57:964–970. doi: 10.1177/0284185115610932.
16. Poulton TB, Murphy WD, Duerk JL, Chapek CC, Feiglin DH. Bone marrow reconversion in adults who are smokers: MR imaging findings. AJR Am J Roentgenol 1993;161:1217–1221. doi: 10.2214/ajr.161.6.8249729.
17. Manceron V, Guignard S, de Broucker F, Paycha F, Pouchot J, Vinceneux P. Bone marrow reconversion and magnetic resonance imaging: case report. Rev Med Interne 2003;24:830–834. doi: 10.1016/j.revmed.2003.08.003.
18. Saadate-Arab M, Troufléau P, Stines J, Verhaeghe JL, Rios M, Molé D. MR imaging findings of bone marrow reconversion induced by growth factors in 3 patients. J Radiol 2002;83 (2 Pt 1):147–152. doi: 10.1097/00004424-200202000-00007.
19. Hirano K, Inoue G. Classification and treatment of hamate fractures. Hand Surg 2005;10:151–157. doi: 10.1142/S0218810405002747.
20. Milch H. Fracture of the hamate bone. J Bone Joint Surg 1934;16:459–462.
21. Carroll RE, Lakin JF. Fracture of the hook of the hamate: acute treatment. J Trauma 1993;34:803–805. doi: 10.1097/00005373-199306000-00009.
22. Takeda S, Tatebe M, Ishii H, Morita A, Wakai K, Hirata H. Computerized tomographic prediction of flexor tendon injuries complicating hamate hook fractures. J Hand Surg Eur Vol 2019;44:367–371. doi: 10.1177/1753193418823503.
23. Nanno M, Sawaizumi T, Ito H. Simplified dorsal approach to fracture of the hamate hook with percutaneous fixation with screws. J Plast Surg Hand Surg 2010;44:214–218. doi: 10.3109/02844310801956714.
24. Cain JE Jr, Shepler TR, Wilson MR. Hamatometacarpal fracture-dislocation: classification and treatment. J Hand Surg Am 1987;12:762–767. doi: 10.1016/s0363-5023(87)80064-3.
25. Ebraheim NA, Skie MC, Savolaine ER, Jackson WT. Coronal fracture of the body of the hamate. J Trauma 1995;38:169–174. doi: 10.1097/00005373-199502000-00004.
26. Wharton DM, Casaletto JA, Choa R, Brown DJ. Outcome following coronal fractures of the hamate. J Hand Surg Eur Vol 2010;35:146–149. doi: 10.1177/1753193408098907.
27. Nunez FA Jr, Luo TD, Jupiter JB, Nunez FA Sr. Scaphocapitate syndrome with associated trans-scaphoid, trans-hamate perilunate dislocation: a case report and description of surgical fixation. Hand (N Y) 2017;12:N27–N31. doi: 10.1177/1558944716668837.
28. Sabat D, Dabas V, Suri T, Wangchuk T, Sural S, Dhal A. Trans-scaphoid transcapitate transhamate fracture of the wrist: case report. J Hand Surg Am 2010;35:1093–1096. doi: 10.1016/j.jhsa.2010.04.023.
29. Schweizer A, Kammer E. Transhamate periscaphoid axial radial fracture dislocation of the carpus. J Hand Surg Am 2008;33:210–212. doi: 10.1016/j.jhsa.2007.11.003.
30. Xiong G, Xiao Z, Wang H, Guo S, Tao J. Microstructural study of the lunate in stage III Kienböck's disease with micro-computed tomography imaging. J Hand Surg Eur Vol 2017;42:71–77. doi: 10.1177/1753193416664502.
31. Sauerland S, Lefering R, Bayer-Sandow T, Brüser P, Neugebauer EA. Fingers, hands or patients? The concept of independent observations. J Hand Surg Br 2003;28:102–105. doi: 10.1016/s0266-7681(02)00360-1.

How to cite this article: Xiao ZR, Zhang WG, Xiong G. Features of intra-hamate vascularity and its possible relationship with avascular risk of hamate fracture. Chin Med J 2019;132:2572–2580. doi: 10.1097/CM9.0000000000000417